Title
Analysis, Implementation, and Application of Acoustic and Seismic Arrays

Permalink
https://escholarship.org/uc/item/3v00c698

Journal
Center for Embedded Network Sensing, 32(6)

Authors
Stafsudd, J.Z
Asgari, Shadnaz
Chen, Chiao-En
et al.

Publication Date
2006-11-20

Peer reviewed

Analysis, Implementation, and Application of Acoustic and Seismic Arrays[1)]

STAFSUDD J Z[1]   ASGARI S[1]   ALI A M[1]   CHEN C E[1]
HUDSON R E[1]   LORENZELLI F[1]   YAO K[1]   TACIROGLU E[2]

[1](*Electrical Engineering Department, Los Angeles, CA* 90095*, USA*)
[2](*Civil and Environmental Engineering Department, Los Angeles, CA* 90095*, USA*)
(E-mail: yao@ee.ucla.edu)

Abstract   In this paper, we consider the analysis, implementation, and application of wideband sources using both seismic and acoustic sensors. We use the approximate maximum likelihood (AML) algorithm to perform acoustic direction of arrival (DOA). For non-uniform noise spectra, whitening filtering was applied to the received acoustic signals before the AML operation. For short-range seismic DOA applications, one method was based on eigen-decomposition of the covariance matrix and a second method was based on surface wave analysis. Two well-known optimization schemes were used to estimate the source locations from the estimated DOAs at sensors of known locations. Experimental estimation of the DOAs and resulting localizations using the acoustic and seismic signals generated by striking a heavy metal plate by a hammer were reported.

Key words   Acoustic array, seismic array, beamforming, DOA, localization

1 Introduction

Distributed sensor networks have been proposed for a wide range of applications. The main purpose of a sensor network is to monitor an area, including detecting, identifying, localizing, and tracking one or more objects of interest. These technological advances not only open up many possibilities but also introduce challenging issues for the collaborative processing of wideband acoustic and seismic signals for source localization and beamforming. In this paper, we briefly review the approximate maximum-likelihood (AML) algorithm for acoustic direction-of-arrival (DOA) and localization in Section 2. Then we describe two methods for seismic source DOA and localization for short-range seismic data in Section 3. In Section 4, we apply two well-known optimization criteria to estimate the seismic source locations from estimated DOAs found at seismic sensors with known locations. Section 5 describes an experiment utilizing both the acoustic and seismic array data for the localization of a heavy metal plate struck by a metal hammer. Localization results based on the two different seismic array methods and the AML acoustic array are compared and shown to be quite accurate. Section 6 includes a brief conclusion.

2 AML algorithm for acoustic source DOA/localization

Suppose we have M wideband sources in the far field. Then for a randomly distributed array of P sensors, the data collected by the pth sensor at time n is given by

$$x_p(n) = \sum_{m=1}^{M} S^{(m)}(n - t_{cp}^{(m)}) + w_p(n), \text{ for } n = 0, ..., N-1, \ p = 1, ..., P, \ m = 1, ..., M \qquad (1)$$

where $S^{(m)}$ is the mth source signal at the array centroid position r_c. $t_{cp}^{(m)}$ is the relative time delay of the mth source to the centroid and pth sensor, w_p is the zero mean white Gaussian noise with variance σ^2. So as a result in frequency domain we would have

$$X(w_k) = D(w_k) * S(w_k) + \eta(w_k), \text{ for } k = 0, ..., N-1 \qquad (2)$$

where $X(w_k) = [X_1(w_k), ..., X_p(w_k)]^{\mathrm{T}}$, $S(w_k)$ is the corresponding frequency spectrum data vector, and $\eta(w_k)$ is the zero mean complex white Gaussian noise with variance $N\sigma^2$. $D(w_k) = [D_1(w_k), ..., D_p(w_k)]^{\mathrm{T}}$, with $D_p(w_k) = [e^{-j2\pi w_k t_{cp}^{(1)}/N}, ..., e^{-j2\pi w_k t_{cp}^{(M)}/N}]^{\mathrm{T}}$, is the $M \times P$ steering matrix. So the maximum

likelihood estimation of the source DOA and source signal are given by the following optimization criterion

$$max_\theta J(\theta) = max_\theta \sum_{k=1}^{N/2} \|P(w_k,\theta)X(w_k)\| = max_\theta \sum_{k=1}^{N/2} tr(P(w_k,\theta)R(w_k)) \tag{3}$$

where $P(w_k,\theta) = D(w_k)D(w_k)^\dagger$. $D^\dagger = (D(w_k)^H D(w_k))^{-1} D(w_k)^H$ is the pseudo-inverse of the steering matrix and $R(w_k) = X(w_k)X(w_k)^H$ is the one snap shot covariance matrix. For more information about the AML refer to [1,2].
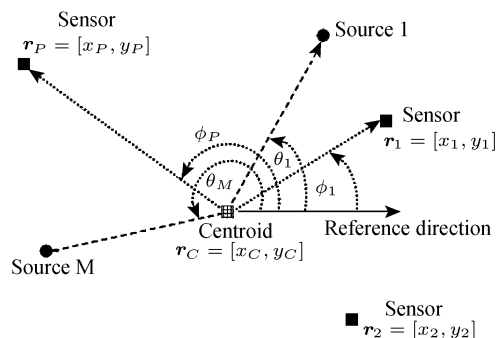

Fig. 1 Far-field notations for sources, sensors and sensor array centroid.

The previously formulated AML algorithm[1,2] has been applied to tracked vehicle and music sources. Modifications were made in this paper for application to a very wideband source. The following subsections describe the modifications.

2.1 Channel whitening for acoustic AML

The first adjustment we made on the AML algorithm is to perform channel whitening. One of the important assumptions in the development of the original AML algorithm is that the noise spectral density in all the channels are uniform. In the real world, the background noise is non-uniform. Thus, one way to reduce the effect of this non-uniformity is by using channel whitening. To do whitening, we first record the background noise when the signal is not present. Then we use this recording to estimate the average power spectral density of the background noise for each microphone channel. Next, the complex-valued spectral amplitude (when the signal is present) is divided by the square root of the average noise power at each frequency and for each microphone channel. This yields the whitened version of the signal in the frequency domain. The whitened version of the signal is then sent to the AML algorithm.

2.2 Frequency bin selection for acoustic AML

The second adjustment we made on the AML algorithm is to implement better frequency bin selection. In the original algorithm, the total power of the received waveform in all the channels was the main criterion in selecting a subset of frequencies to do maximum likelihood criterion estimation. From experience, we know that most of the useful information in the signal are stored in the higher frequencies, while the background noise (such as wind noise), is more concentrated in the low frequencies. In order to obtain a better estimate, after computing the complex amplitude in each channel and normalizing by the noise spectrum, the square magnitudes are summed over all channels and this sum is multiplied by the square of the frequency of the bin. Consequently we put more weight in the higher frequencies of the received data. Furthermore, when a collection of local maxima of these weighted square magnitudes in the frequency domain are close to each other, we select only a representative bin in the AML algorithm for further processing.

3 Two methods for seismic source DOA estimation

Previous work[3~5] in the area of seismic DOA and source localization was done in an environment where the sensor and source were hundreds to thousands of kilometers apart. In our field experiments, coherent seismic and acoustic data was collected from sensors and sources less than 100 meters apart. Direction of arrival (DOA) and source localization results using seismic data are compared to and

supplement similar results using acoustic data. The seismic data collected from our experiments is considered to be short-range data compared to the previous work. Short-range seismic data exhibits different behavior and composition than long-range data, hence it poses unique challenges for seismic DOA/source localization estimation.

Long-range seismic signal from a seismic event contain P and S body waves and Rayleigh and Love surface waves, each type of wave exhibit frequency content and velocity different from others. In the long-range scenario, the earth acts as a frequency and velocity filter such that P, S, Rayleigh and Love waves are well-separated in the frequency domain and on the arrival time-line. Surface waves (Rayleigh and Love) dominate the short-range seismic signal with negligible body wave. In the short-range scenario, the Love and the Rayleigh waves are almost completely overlapping. Rayleigh wave exhibits a rolling motion in the direction of propagation, occupying the vertical direction (the direction perpendicular to the ground) and the direction of propagation in the ground plane. Love wave produces side-to-side motion perpendicular to the direction of propagation in the ground plane.

3.1   Event detection for seismic DOA estimation

In the field, many events can contribute to seismic readings. To accurately determine DOA and locate the source of an event of interest, discrimination against other interfering seismic sources is important.

The simple scheme developed for event detection involves first dividing the collected record into time windows of N samples where an event can be well-contained. Time-sampled acceleration signal in $x-$, $y-$, and z–directions is collected at triaxial seismic stations and organized into column vectors

$$
\begin{aligned}
\boldsymbol{x}_x &= \left[\begin{array}{cccc} x_x\left(k\right) & x_x\left(k+1\right) & \cdots & x_x\left(k+N-1\right) \end{array} \right]^{\mathrm{T}} \\
\boldsymbol{x}_y &= \left[\begin{array}{cccc} x_y\left(k\right) & x_y\left(k+1\right) & \cdots & x_y\left(k+N-1\right) \end{array} \right]^{\mathrm{T}} \\
\boldsymbol{x}_z &= \left[\begin{array}{cccc} x_z\left(k\right) & x_z\left(k+1\right) & \cdots & x_z\left(k+N-1\right) \end{array} \right]^{\mathrm{T}}
\end{aligned}
\tag{4}
$$

where the time indices k and N denote the beginning and the extent of a time window, respectively, which contains an event of interest. These vectors form the columns of the $(N \times 3)$ the signal matrix (for each window) given by $\boldsymbol{X} = [\, \boldsymbol{x}_x \;\; \boldsymbol{x}_y \;\; \boldsymbol{x}_z \,]$. A sample covariance matrix is formed from zero–mean data at each window: $\boldsymbol{M} = (\boldsymbol{X} - E\{\boldsymbol{X}\})^{\mathrm{T}}(\boldsymbol{X} - E\{\boldsymbol{X}\})$. We perform eigen-decomposition on the sample covariance matrix, $\boldsymbol{M}$: $\boldsymbol{M} * \boldsymbol{V} = \boldsymbol{V} * \boldsymbol{D}$ where $\boldsymbol{V} = \left[\begin{array}{ccc} \boldsymbol{v}_1 & \boldsymbol{v}_2 & \boldsymbol{v}_3 \end{array} \right]$ contain the eigenvectors $\boldsymbol{v}_i = \left[\begin{array}{ccc} x_i & y_i & z_i \end{array} \right]^{\mathrm{T}}$, and $\boldsymbol{D} = \mathrm{diag}\left(\lambda_1, \lambda_2, \lambda_3\right)$ contain the eigenvalues, from the smallest to the largest. The eigenvalues of the sample covariance matrix as a function of window number gives an indication of the signal energy contained in each window as a function of time. The size of the eigenvalues of each sample covariance matrix is a good indicator of the presence of a seismic event of interest. This simple process can be performed on sliding time windows across the entire data record. Because of the lower sampling rate, a plot of the three eigenvalues as a function of time suppresses the temporal details of the raw waveforms while heightening the sensitivity to a waveform that is coherent in all three channels.

3.2   Seismic DOA estimation *via* covariance matrix analysis

Method 1 uses the eigen-decomposition of the covariance matrix. It utilizes the previously published method of polarization analysis[3] applied to long-range seismic data to our collected short-range data. The eigen-decomposition of the covariance matrix formed by data from a window containing an event of interest provides a means to estimate the DOA of the event. The largest eigenvalue, λ_3 corresponds to the average energy of the strongest seismic mode polarized in the direction of the corresponding eigenvector, v_3 ; the other two eigenvalues and their corresponding eigenvectors describe other seismic modes whose polarizations are mutually orthogonal. Rayleigh wave is elliptically polarized and occupy two orthogonal directions. Love wave is rectilinearly polarized in the direction orthogonal to the direction of propagation. From each eigenvector, the azimuth and depression angles are calculated by $Az_i = \arctan\left(y_i/x_i\right)$ and $Dep_i = \arctan\left(z_i \big/ \sqrt{x_i^2 + y_i^2}\right)$. The azimuth angle is defined as the angle measured from the x-axis, counter-clockwise on the ground plane; and the depression angle is defined as the angle measured from the x-y plane at the height of the sensor to the source, down being positive. The eigenvectors of the covariance matrix define a rotation of the triaxial data into its principle

components, but do not define a specific direction. The azimuth angles found from components of an eigenvector has a 180-degree ambiguity. Our results suggest that the Rayleigh wave dominates in energy compared to the Love wave in our data, hence the azimuth angle found from components of v_3 gives the estimate of the DOA. If the Love wave dominates in energy instead, the azimuth angle found from components of v_3 gives an angle perpendicular to the DOA.

3.3 Seismic DOA estimation *via* surface wave analysis

Method 2 is based on the surface wave analysis. From the inherent behavior of Rayleigh and Love waves, it is clear that the Rayleigh wave is polarized in two mutually orthogonal directions in the three-dimensional space, and Love wave is polarized orthogonally to both directions of the Rayleigh wave. The three-dimensional Cartesian space can hence be rotated such that two channels pick up the Rayleigh wave, and one other, orthogonal channel picks up only the Love wave. In the ideal situation where the triaxial sensor is inserted in such a way that we assume no leakage exists between the z-direction and the ground plane, all the motion in the vertical direction (z) is due to the Rayleigh wave. The other component of the Rayleigh wave and the direction of motion of the Love wave are perpendicular to each other, and are both in the ground plane.

Rayleigh wave exhibits an elliptical motion in the plane made-up by the vertical axis (z) and the direction of propagation projected onto the ground plane (p). The equation of an ellipse in the z-p plane is $z^2/A^2 + p^2/B^2 = 1$. If the time waveform of the ellipse in the p-direction is $p(t) = B\sin(t)$, the time waveform of the ellipse in the z-direction is then $z(t) = A\cos(t)$. It is then clear that the signals due to Rayleigh wave in the z- and p-directions are 90 degrees out of phase; and that the derivative of the signal in the p-direction is in phase with and proportional to the z-direction signal. Assuming no leakage of accelerations in the ground plane into the z-direction signal, all motion in the z-direction is due to Rayleigh wave. It then follows that the projection of the integral of the vertical acceleration (z-direction collected signal) onto the ground plane depicts the Rayleigh wave component in the ground plane. Mathematically, the integral of the vertical acceleration, $\mathbf{vel}_z = \int \boldsymbol{x}_z \mathrm{d}t$ dotted with the signals collected in the x- and y-directions

$$corrX = \mathbf{vel}_z{}^{\mathrm{T}} * \boldsymbol{x}_x, \quad corrY = \mathbf{vel}_z^{\mathrm{T}} * \boldsymbol{x}_y \tag{5}$$

explicitly (without ambiguity) defines the direction of propagation of the Rayleigh wave in the ground plane. The direction of the Love wave motion is the vector in the ground plane orthogonal to that of the Rayleigh wave

$$\mathbf{dirRay} = \begin{bmatrix} corrX & corrY \end{bmatrix}^{\mathrm{T}}, \quad \mathbf{dirLov} = \begin{bmatrix} -corrY & corrX \end{bmatrix}^{\mathrm{T}} \tag{6}$$

4 Seismic source localization *via* estimated DOAs

For the purpose of seismic source localization using estimated DOAs at sensors of known locations, the objective is to find the point in the x–y plane that's closest to lines formed by the estimated DOAs at all sensors. We first define the distance d_m between an arbitrary point $[x, y]$ and the line formed by the estimated DOA at the m_{th} seismic sensor as illustrated in Fig. 2. The m_{th} sensor is located at $[x_m, y_m]$. The unit vector along the estimated DOA ν_m found at sensor m is $[\cos(\nu_m)\sin(\nu_m)]^{\mathrm{T}}$, the unit vector along the direction perpendicular to the line formed by the estimated DOA, ν_m, is $[-\sin(\nu_m)\cos(\nu_m)]^{\mathrm{T}}$. The distance between a point in the x–y plane, $[x, y]$, and the estimated DOA line through sensor m along ν_m is defined as the projection of the difference vector between $[x, y]$ and the location of the m_{th} sensor onto the direction $[-\sin(\nu_m)\cos(\nu_m)]^{\mathrm{T}}$.

$$d_m = \left| \begin{bmatrix} -\sin(\nu_m) \\ \cos(\nu_m) \end{bmatrix}^{\mathrm{T}} \left(\begin{bmatrix} x_m \\ y_m \end{bmatrix} - \begin{bmatrix} x \\ y \end{bmatrix} \right) \right|$$
$$d_m = |\cos(\nu_m) \cdot (y_m - y) - \sin(\nu_m) \cdot (x_m - x)| \tag{7}$$

The following subsections describe formulation of two well-known criteria to serve the needs of source localization using DOA estimates.

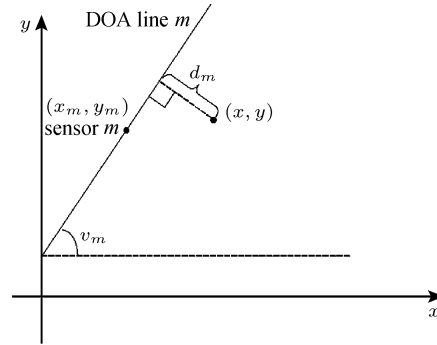Fig. 2 Source localization illustration

4.1   A weighted $L2$ norm approach

The first optimization criterion for source localization via DOAs at sensors of known locations is the $L2$ norm criterion. It is employed to formulate the optimization problem because it is robust to measurement noises. We want to minimize the sum of the distance from the point $[x,\ y]$ to all lines formed along the estimated DOAs, namely

$$\min_{(x,y)} \sum_{m=1}^{numSensor} |d_m|^2 \tag{8}$$

The uncertainties in the estimated DOAs, δ_m, translate into uncertainties in the location with the distance between the location of sensor m and the point $[x,\ y]$. The term

$$\delta_m \cdot \left\| \begin{bmatrix} x_m - x \\ y_m - y \end{bmatrix} \right\| \tag{9}$$

is a small-angle approximation of the uncertainties in the m_{th} estimate of location at sensor m, with a DOA uncertainty of δ_m, to the point in question, $[x,\ y]$. The larger this term is, the larger the uncertainty. It then follows that if each term in the sum in the $L2$ norm criterion is weighted by the inverse of the above term, more accurate estimate of the location of the source can be obtained. The weighted $L2$ optimization for seismic source localization is

$$\min_{(x,y)} \sum_{m=1}^{numSensor} \frac{d_m^2}{\delta_m^2 \cdot \left\| \begin{bmatrix} x_m - x \\ y_m - y \end{bmatrix} \right\|^2} \tag{10}$$

4.2   A weighted $L1$ norm approach

$L1$ norm criterion is in general more robust to outliers than the $L2$ norm criterion. $L1$ norm criterion may perform better in cases where the estimated DOA at some sensors are highly inaccurate. The $L1$ norm criterion defines the optimization problem as follows

$$\min_{(x,y)} \sum_{m=1}^{numSensor} |d_m| \tag{11}$$

In the same logic as explained in Section 4.1 given above, weighting each term in the sum in the $L1$ criterion helps the estimation stay accurate in case of largely uncertain DOA estimates. The weighted $L1$ norm optimization for seismic source localization is

$$\min_{(x,y)} \sum_{m=1}^{numSensor} \frac{d_m}{\delta_m \cdot \left\| \begin{bmatrix} x_m - x \\ y_m - y \end{bmatrix} \right\|} \tag{12}$$

5   Application to acoustic/seismic source localization

We conducted a series of acoustic and seismic experiments at Garner Valley, CA. Six triaxial (labelled 1 to 6) and three biaxial (labelled 7 to 9) accelerometer sensors were placed in a regular manner as shown in Fig. 3. In addition, two microphone arrays were also placed in the middle of the square bounded by sensors 2,5,6,3 and 4,7,8,5 labelled as Array2 and Array1 and shown as two squared symbols both in the left hand side and its exploded view in the right hand side of Fig. 3. A large heavy metal plate was placed in the middle of the square bounded by the accelerometers 1,4,5,2. The metal plate is situated at the location of (7.62,22.86). In the experiment, a person struck the plate with a heavy hammer. A series of twelve bangs, three horizontal bangs, followed by three vertical bangs, then repeated again were made. Acoustic and seismic signals from only the vertical bangs are used in the following acoustic (first three bangs) and seismic (all six bangs) processing.
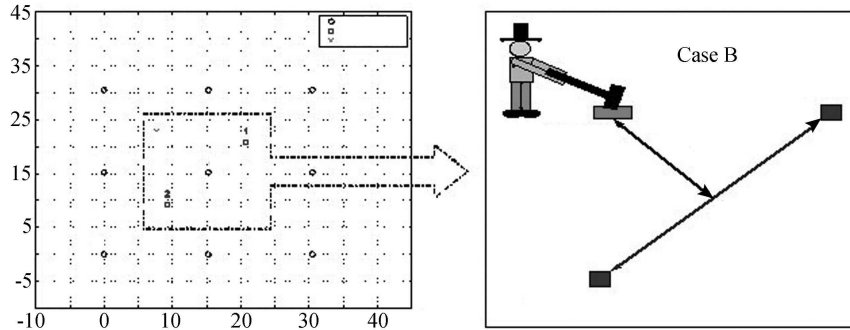

Fig. 3   Sensor/source locations in Garner Valley experiments

5.1   Acoustic source localization results using AML

First, consider the acoustic waveforms. Fig. 4 shows the power spectrum of the received acoustic hammered signal. Due to the non-uniformity of the spectra of the received acoustic hammered signal,
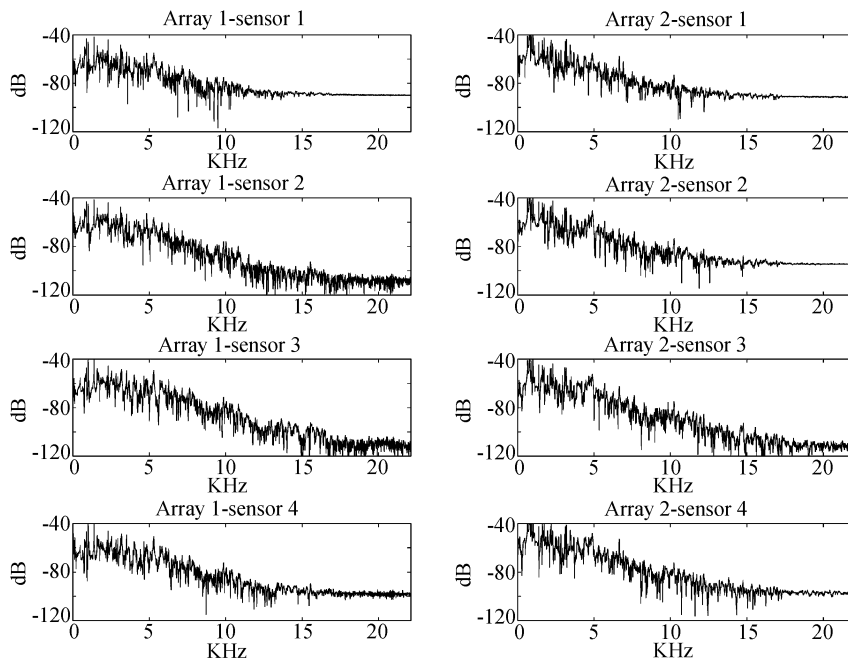

Fig. 4   Spectra of 8 received hammered acoustic signals
received hammering signal in frequency domain from array 1 and array 2 signals

a whitening operation using the noise power spectrum during the quiet period (in the absence of hammering), was performed on the original received hammered signal. The spectra of the whitened signals are shown in Fig. 5, and these signals are used by the AML DOA algorithm which assumes a white noise spectrum. From the bearing crossing of these two estimated DOAs, the estimated plate location using the acoustic array data is given by (7.25, 24.4), which is also quite close to the true plate location of (7.62, 22.86).
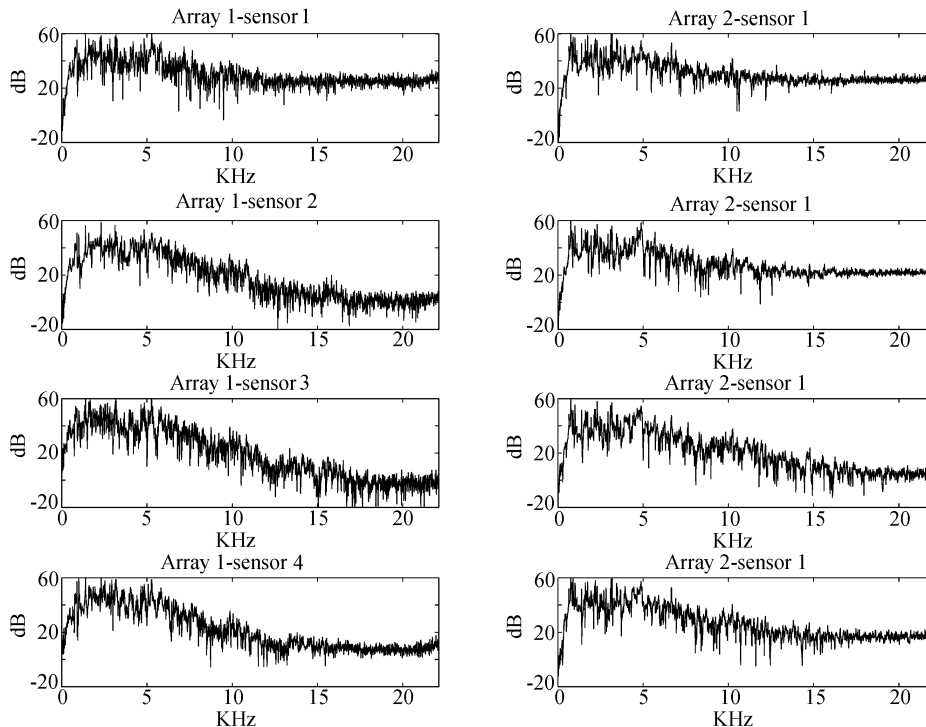

Fig. 5 Spectra of 8 whitened received hammered acoustic signals
The normalized version of the received signal in frequency domain from array 1 and array 2

5.2   Seismic source localization results

The seismic DOA schemes used six seismic strikes sampled at 200 Hz. A sample collected signal at sensor 1 is shown on the left half of Fig. 6. The right half of Fig. 6 shows the eigenvalue plot as a function of window number used for event detection. The windows with maximum eigenvalue above $-40dB$ are declared to contain an event of interest. Using method 1, the left half of Table 1 shows the directional angles from the six triaxial sensors and these results are plotted on the left half of Fig. 7. From the method 1 estimated DOAs tabulated on the left half of Table 1, it seems sensor $3's$ estimate is rotated about 90 degree from the true propagation direction. This result perhaps is due to the fact that for this sensor, the Love wave component is stronger than the Rayleigh wave component, whose movement is known to be perpendicular to the propagation direction. All other estimated DOAs point in the general direction of the true source. Using method 2, the right half of Table 1 shows these estimated propagation angles and are plotted on the right half of Fig. 7. All DOAs found by method 2 are in the general direction of the true location of the plate. Unlike the result from method 1, the propagation angle of sensor 3 using method 2 appears to be correct now. Table 2 shows the results of seismic source localization using both un-weighted and weighted $L2$ norm and $L1$ norm criteria. We noticed that weighted criteria performed better than their un-weighted counter-parts in all cases. Weighting significantly improved the source localization results using estimated DOAs from method 1. While all weighted results are fairly close to the true source location, $L2$ norm criterion performed better than the $L1$ norm criterion.

A simple fusion of the two seismic localization results with the acoustic localization result, by direct

averaging yields a fusion-based estimated plate location of (7.82, 23.99). At least for this experiment, the fusion-based localization result shows an improvement to the localization results without the fusion. Clearly, more sophisticated fusion operations can be used and should yield better results in most cases.
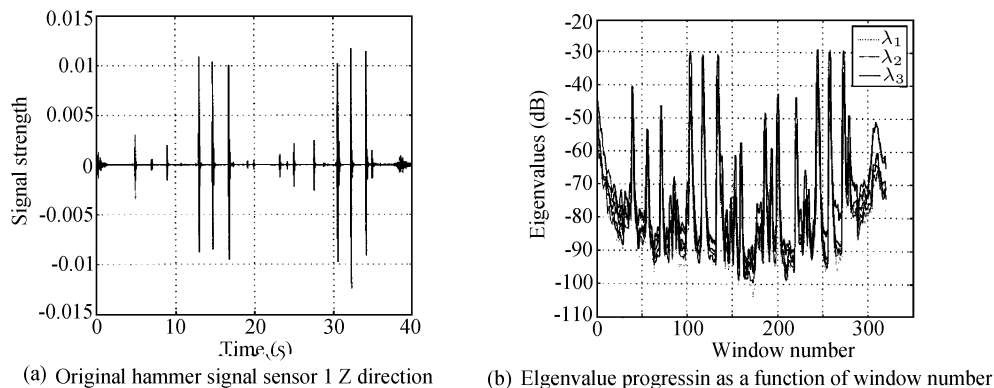

(a) Original hammer signal sensor 1 Z direction

(b) Elgenvalue progressin as a function of window number

Fig. 6 Seismic event detection results

Table 1   Azimuth angles (degrees) using methods 1 and 2

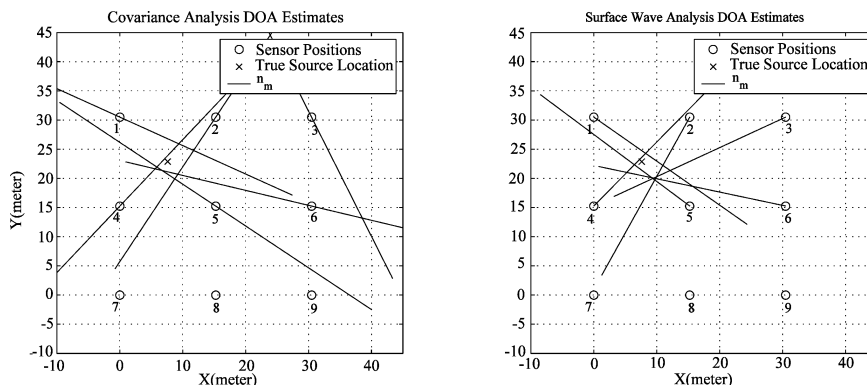| StkNo.	1	2	3	4	5	6	Aver.	SD	1	2	3	4	5	6	Aver.	SD
Snsr1	-23	-27	-26	-26	-26	-27	-26.0	1.33	-38	-39	-37	-38	-36	-35	-37	1.48
Snsr2	57	57	60	59	58	59	58.4	1.02	-119	-119	-116	-116	-118	-115	-117	1.49
Snsr3	-77	-80	-63	-61	-42	-68	-65.0	13.8	-153	-154	-151	-157	-156	-149	-154	3.17
Snsr4	48	48	49	49	49	49	48.7	0.39	47	48	48	48	48	48	48	0.38
Snsr5	-30	-35	-36	-40	-37	-37	-35.6	3.31	142	142	141	141	140	142	141	0.88
Snsr6	-11	-16	-16	-14	-18	-11	-14.4	2.80	165	167	168	168	167	169	167	1.47

Fig. 7 Seismic DOA estimation using methods 1 and 2

Table 2   Seismic source localization results

Loc. (m)	True Loc.	Unw. $L2$	Wt. $L2$	Unw. $L1$	Wt. $L1$
Mth.1 X	7.62	15.98	9.39	11.70	9.48
Mth.1 Y	22.86	24.30	24.82	24.76	25.86
Mth.2 X	7.62	9.11	8.40	9.49	8.22
Mth.2 Y	22.86	21.22	23.58	20.03	24.28

6 Conclusions

In this paper, we considered the use of the AML algorithm to perform acoustic DOA. For non-uniform noise spectra, whitening filtering was applied to the received acoustic signals before the AML

operation. For short-range seismic DOA applications, one method was based on eigen-decomposition of the covariance matrix and a second method was based on surface wave analysis. The weighted $L2$ norm and weighted $L1$ norm criteria were applied to estimated seismic DOAs to obtain the estimated seismic source location. Experimental estimation of the DOAs and resulting localizations using the acoustic and seismic signals generated by striking a heavy metal plate by a hammer were reported. Both the acoustic and seismic source localization results based on the proposed methods were fairly accurate. We intend to perform more complex experiments as well as to perform a comprehensive literature survey to identify seismic source localization methods for short and very-short ranges.

References

1 Chen J, Hudson R E, Yao K. Maximum-likelihood source localization and unknown sensor location estimation for wideband signals in the near-field. *IEEE Transactions in Signal Processing*, 2002, **50**(8): 1843∼1854

2 Chen J, Yip L, Elson J, Wang H, Maniezzo D, Hudson R E, Yao K, Estrin D. Coherent acoustic array processing and localization on wireless sensor network. *Proceedings of the IEEE*, 2003, **91**(8): 1154∼1162

3 Kirlin R L, Done W L. Covariance analysis for seismic signal processing. Society of Exploration Geophysicists, 1999. SEG Monograph, 1999. 69∼83

4 Magotra N, Ahem N, Chael E. Single-station seismic event detection and localization. *IEEE Transactions on Geoscience and Remote Sensing*, 1989, **27**(1): 15∼23

5 Flinn E, Signal analysis using rectilinearity and direction of particle motion. *Proceedings of the IEEE on Teleseismic Signal Data Techniques*, 1965, **53**(12): 1874∼1876

STAFSUDD J Z   Ph. D. candidate in the EE Department at UCLA. Her research interests include seismic source localization, sensor array processing, and sensor fusion.

ASGARI S   Ph. D. candidate in the EE Department at UCLA. Her research interests include acoustic source localization, sensor array processing, and sensor system performance.

ALI A M   Ph. D. candidate in the EE Department at UCLA. His research interests are source localization, signal and array processing, and sensor network.

CHEN C E   Ph. D. candidate in the EE Department at UCLA. His research interests include acoustic source localization, array signal processing, and particle filters.

HUDSON R E   Consultant and research associate in the EE Department at UCLA. His research interests are signal and array processing, and radar system design and signal processing.

LORENZELLI F   Research and innovation manager at ST Microelectronics and researcher in residence at UCLA. His research interests include signal and array processing, sensor networks, and wireless communications.

YAO K   Professor in the EE Department at UCLA. His research interests include signal and array processing, sensor networks, and wireless communication.

TACIROGLU E   Assistant professor in the CEE Department at UCLA. His research interests include solid and structural mechanics, inverse problems, and smart structures and active material systems.